



## **Analytical and Numerical Studies for the Evaluation of Higgs Boson Pair Production via Gluon Fusion**

Kay Schönwald, Technische Universität Dortmund, Germany

September 8, 2015

The amplitudes and cross sections for higgs pair production to gluon fusion are studied analytically and numerically to verify the usability of the implemented code and to get a deeper understanding for splitting graphs, which are needed to describe double parton interaction at small transverse separation.

# Contents

<b>1. Introduction</b>	<b>3</b>
<b>2. Theory</b>	<b>3</b>
2.1. Single and Double Parton Scattering . . . . .	3
2.2. Double Counting Problem . . . . .	4
<b>3. Analytical Studies</b>	<b>5</b>
3.1. Mathematical Tools . . . . .	5
3.2. Explicit Imaginary Part . . . . .	5
3.3. Small $p_T$ -Limit . . . . .	6
<b>4. Numerical Studies</b>	<b>7</b>
4.1. Numerical Stability . . . . .	7
4.2. Cross Check with $m_q$ -Expansion . . . . .	16
4.3. Cross Check with $p_T$ -Expansion . . . . .	25
4.4. Results . . . . .	27
<b>5. Conclusion</b>	<b>28</b>
<b>A. Kinematic Variables</b>	<b>29</b>
<b>B. Evaluation of the Imaginary Part</b>	<b>29</b>

# 1. Introduction

The interaction between two hadrons at high energies is described by the parton model. Here all partons, namely quarks and gluons, in the hadron are considered non interacting. So every interaction between two partons is independent of the proton background and the only non perturbative input is the probability to find a parton  $i$  with a certain momentum  $x_i$ , described by parton distribution functions (PDFs), which were for example measured at Hera (DESY) and are well known.

With the high energies reached by the LHC, more than one parton of one hadron can have a hard interaction with a parton of the other hadron, producing particles with large mass or transverse momentum. At small transverse separation this contributions are double counted with loop level corrections to single parton scattering.

The purpose of my work was to study the amplitudes for gluon fusion into a higgs boson pair at one loop level given in [5], analytically and numerically, to get deeper insight into this contributions for double parton scattering (DPS).

In the first part the analytical structure of the imaginary part is studied and an analytical expression for the small transverse momentum limit is given.

The second part focuses on the numerical evaluation of the transition amplitude. Numerical stability is tested and the implementation is cross checked with the small quark mass limit given in [4] and the limit for small transverse momentum is given.

## 2. Theory

### 2.1. Single and Double Parton Scattering

Making use of the 'Parton Model' single parton scattering in hadron interactions can be described via the formula

$$\frac{d^2\sigma_{\text{single}}}{dx_1 d\bar{x}_1} = F(x_1) F(\bar{x}_1) \sigma(x_1, \bar{x}_1),$$

where  $F(x_i)$  describe the single parton distribution functions (sPDF) and  $x_1, \bar{x}_1$  the momentum fractions of the scattering partons. Following this path and assuming factorisation between the two hard scattering events in double parton scattering (DPS) one arrives at the cross section formula

$$\frac{d^4\sigma_{\text{double}}}{dx_1 d\bar{x}_1 dx_2 d\bar{x}_2} = C \frac{d^2\sigma_1(x_1, \bar{x}_1)}{dx_1 d\bar{x}_1} \frac{d^2\sigma_2(x_2, \bar{x}_2)}{dx_2 d\bar{x}_2} \int d^2y F(x_1, x_2, y) F(\bar{x}_1, \bar{x}_2, y).$$

Here  $F(x_1, x_2, y)$  describe double parton distributions (DPD) and can be interpreted as the probability to find a pair of partons with momentum fraction  $x_1$  and  $x_2$  and a transverse separation  $y$ .  $x_1, x_2$  describe the momentum fractions of the partons in one hadron and  $\bar{x}_1, \bar{x}_2$  the momentum fractions in the other hadron.

The DPD therefore have to include all non perturbative information of parton correlations inside the proton and are generally not known. To obtain further results simple assumptions and approximations can be made. The simplest yields to the 'Pocket Formula'

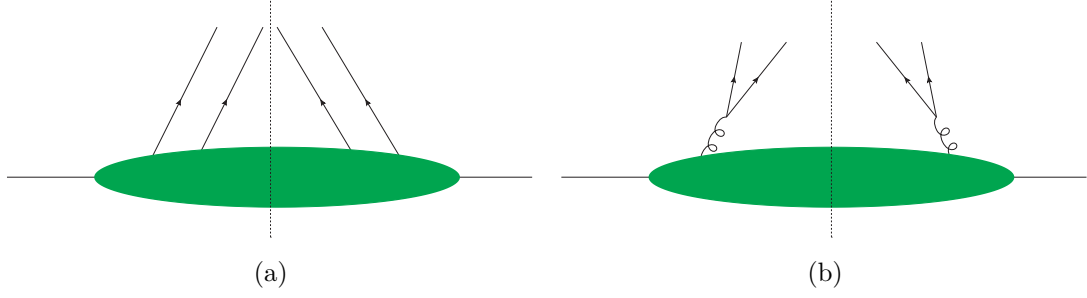


Figure 1: Graphical illustration for: a DPS and b DPS at small transverse momentum

for DPS, here it is assumed that the DPD factorises into two sPDF and a transverse distribution function

$$F(x_1, x_2, y) \approx F(x_1)F(x_2)G(y).$$

Then the DPD cross section can be easily obtained by

$$\frac{d^4\sigma_{\text{double}}}{dx_1 d\bar{x}_1 dx_2 d\bar{x}_2} = \frac{C}{\sigma_{\text{eff}}} \frac{d^2\sigma_1(x_1, \bar{x}_1)}{dx_1 d\bar{x}_1} \frac{d^2\sigma_2(x_2, \bar{x}_2)}{dx_2 d\bar{x}_2}$$

with  $\sigma_{\text{eff}} = 1/\int d^2b G(b)$  and  $C$  an symmetry factor.

Although this simple approximation is in good agreement with experimental findings and used in current analysis and background estimations (see i.e. [1]), this approximation obviously has to break down at some point.

On the one hand the simple factorisation ansatz does not conserve momentum because it has contributions from  $x_1 + \bar{x}_1 > 1$ , on the other hand correlations between partons can only be neglected for small momentum transfers  $x_i$ . Because of the sheer number of sea quarks and gluons, correlations between two partons have to wash out here. For a more detailed discussion see for example [3].

## 2.2. Double Counting Problem

At small transverse separation  $y$  the DPD is dominated by the splitting of one parton. The short distance behaviour of this DPD are proportional to  $1/y^2$  and yield therefore to UV divergent cross sections. This can be understood as a double counting of single parton scattering at one loop level and DPS with splitting.

A possible solution to this problem is to subtract the double counted contributions. In order to do this a good understanding of the loop contributions is necessary. Therefore the next part of this paper focuses on the study of the results of [5] for gluon fusion into a higgs boson pair. For further studies of DPS a large amount of the results can also be applied to Z-boson pair production given in [4].

### 3. Analytical Studies

#### 3.1. Mathematical Tools

To study the analytical expression of the amplitude in [5], the relation

$$\ln(y + i\varepsilon) = \ln(|y|) + i\theta(-y)\pi \quad (3.1)$$

for the branch cut is important.

Therefore the imaginary part of the dilogarithm

$$\text{Li}_2(z) = - \int_0^1 \frac{\ln(1-zt)}{zt} dt \quad (3.2)$$

becomes

$$\text{Im}(\text{Li}_2(y + i\varepsilon)) = \pi\theta(y-1)\ln(y). \quad (3.3)$$

For further informations on polylogarithms see [2]. So the imaginary part of the amplitude can be extracted analytically.

#### 3.2. Explicit Imaginary Part

The imaginary part of every 3- and 4-point function can now be evaluated explicitly. Following every imaginary part is given, the kinematic explanation can be found in B. Mostly the definitions of [5] are used for kinematic variables, which are also summarised in A. When other variables are used, they are defined in the text.

$C(p_1, p_2)$ :

$$\frac{\text{Im}(C(p_1, p_2))}{\pi} = -\frac{1}{s} \ln\left(\frac{z'_1}{z'_2}\right) \quad (3.4)$$

with

$$z'_1 = \frac{1}{2} \left( 1 + \sqrt{1 - \frac{4m_q^2}{s}} \right), \quad z'_2 = 1 - z'_1 \quad (3.5)$$

$C(p_1, p_3)$ :

$$\frac{\text{Im}(C(p_2, p_3))}{\pi} = \frac{1}{t - m_H^2} \ln\left(\frac{z_1}{z_2}\right) \quad (3.6)$$

with

$$z_1 = \frac{1}{2} \left( 1 + \sqrt{1 - \frac{4m_q^2}{m_H^2}} \right), \quad z_2 = 1 - z_1 \quad (3.7)$$

$C(p_2, p_3)$  is obtained by exchanging  $t$  with  $u$ .

$C(p_3, p_4)$ :

$$\frac{\text{Im}(C(p_3, p_4))}{\pi} = -\frac{1-\alpha}{s(1+\alpha)} \left( \ln \left( \frac{y_0 - z_2}{y_0 - z_1} \right) - \ln \left( \frac{y'_0 - z'_2}{y'_0 - z'_1} \right) \right) \quad (3.8)$$

$D(p_1, p_3, p_2)$ :

$$\frac{\text{Im}(D(p_1, p_3, p_2))}{\pi} = \ln \left( \frac{x_+ - z_2}{x_+ - z_1} \right) - \ln \left( \frac{x_+}{x_+ - 1} \right) - \ln \left( -\frac{x_-}{x_+} \right) \quad (3.9)$$

$D(p_1, p_2, p_3)$ :

$$\begin{aligned} \frac{\text{Im}(D(p_1, p_2, p_3))}{\pi} = & -\ln \left( \frac{\beta_1 + y_{1+} - 1}{y_{1+}} \right) + \ln \left( 1 + \frac{\beta_1 - 1}{y_{1+}} \right) \\ & + \ln \left( 1 - \frac{1}{\beta_2 + y_{2-}} \right) + \ln \left( 1 + \frac{\beta_2 - 1}{y_{2-}} \right) \\ & - \ln \left( 1 - \frac{\beta_2}{y_{2-}} \right) + \ln \left( \frac{\frac{y_{1+}}{1-\beta_1} - z_1}{\frac{y_{1+}}{1-\beta_1} - z_2} \right) \\ & + \ln \left( \frac{\frac{y_{1-}}{1-\beta_1} - z_2}{\frac{y_{1-}}{1-\beta_1} - z_1} \right) - \ln \left( \frac{y_{2+} + \beta_2 - z'_1}{y_{2+} + \beta_2 - z'_2} \right) \\ & + \ln \left( \frac{y_{2-} + \beta_2 - z'_1}{y_{2-} + \beta_2 - z'_2} \right) + \ln \left( \frac{\frac{y_{2+}}{1-\beta_2} - z_2}{\frac{y_{2+}}{1-\beta_2} - z_1} \right) \\ & - \ln \left( \frac{\frac{y_{2-}}{1-\beta_2} - z_2}{\frac{y_{2-}}{1-\beta_2} - z_1} \right) - \ln \left( \frac{\frac{y_{2+}}{\beta_2} - z_2}{\frac{y_{2+}}{\beta_2} - z_1} \right) + \ln \left( \frac{\frac{y_{2-}}{\beta_2} - z_2}{\frac{y_{2-}}{\beta_2} - z_1} \right) \end{aligned} \quad (3.10)$$

$D(p_1, p_2, p_3)$  is obtained by exchanging  $t$  with  $u$ .

### 3.3. Small $p_T$ -Limit

In [4] the limits for small quark masses  $m_q$  are given. In the following chapter the limits for small transverse momentum  $p_T$  and small quark mass  $m_q$  are given and it is shown whether these two limits commute or not. The three-point functions  $C(p_1, p_2)$  and  $C(p_3, p_4)$  do not depend on  $p_T$  and are therefore not considered.

$$\begin{aligned} \lim_{m_q \rightarrow 0} \lim_{p_T \rightarrow 0} D(p_1, p_3, p_2) = & \frac{1}{m_H^4} \left( -\ln \left( \frac{m_q^2}{m_H^2} \right) + 1 + \frac{\beta}{2} \ln \left( \frac{s - 2m_H^2 - sv}{s - 2m_H^2 + sv} \right) \right) \\ & + i\pi \left( \frac{p_T^2}{6sm_q^4} + \frac{1}{sm_q^2} - \frac{2}{sm_H^2} + \frac{p_T^2}{sm_H^4} \right) \end{aligned} \quad (3.11)$$

Comparing with

$$\lim_{p_T \rightarrow 0} \lim_{m_q \rightarrow 0} D(p_1, p_3, p_2) = -\frac{4i\pi}{sp_T^2} \ln \left( \frac{m_q^2}{p_T^2} \right) \quad (3.12)$$

shows that for the crossed box (see figure 2c) the limits do not commute. This is due to the dependence on the kinematic variables  $x_{\pm}$ . The term

$$\frac{\sqrt{p_T^2 + 4m_q^2}}{p_T}$$

contained in them has obviously completely different limits depending on the succession. Physically this corresponds to the poles of the propagators occurring at  $p_T = 0$  for massless particles, which can both be on shell. This is not possible for the gluon splitting into two massive particles, resulting in an amplitude without logarithmic divergence. The crossed box is the only term which has this property. The expressions for the other functions are

$$\begin{aligned} \lim_{m_q \rightarrow 0} \lim_{p_T \rightarrow 0} \text{Re}(C(p_1, p_3)) &= -\frac{\ln\left(\frac{2m_q^2}{-2m_H^2 + s - sv}\right) - \ln\left(\frac{m_q^2}{m_H^2}\right) + \pi^2}{s - sv} \\ &= \frac{\ln\left(\frac{2m_H^2}{-2m_H^2 + s - sv}\right) \left[\ln\left(\frac{2m_q^2}{m_H^2}\right) + \ln\left(\frac{m_q^2}{m_H^2}\right)\right] + \pi^2}{s - sv} \\ &= \lim_{p_T \rightarrow 0} \lim_{m_q \rightarrow 0} \text{Re}(C(p_1, p_3)), \end{aligned} \quad (3.13)$$

$$\begin{aligned} \lim_{m_q \rightarrow 0} \lim_{p_T \rightarrow 0} \text{Im}(C(p_1, p_3)) &= \frac{2\pi}{s - s\sqrt{1 - \frac{4m_H^2}{s}}} \ln\left(\frac{m_q^2}{m_H^2}\right) \\ &= \lim_{p_T \rightarrow 0} \lim_{m_q \rightarrow 0} \text{Im}(C(p_1, p_3)). \end{aligned} \quad (3.14)$$

For the straight box  $D(p_1, p_2, p_3)$  the series in  $p_T$  and  $m_q$  do also commute, because the only dependence on  $m_q$  and  $p_T$  is the kinematic variable  $Y$ , which is only dependent on the product  $m_q^2 \cdot p_T^2$ , the Mandelstam variables, which have a finite limits for  $p_T \rightarrow 0$  and term like  $m_q^2/u(t)$ , for which the limits also commute.

This is also verified in the section 4.2 where the implementation for the  $m_q$  limit gives good results even for vanishing  $p_T$ .

## 4. Numerical Studies

### 4.1. Numerical Stability

To check the usability of the implemented code, it is important to study the numerical stability, because a number of term in the formulas in [5] can encounter numerical problems.

To study the stability the 3- and 4-point function were plotted against the ratio  $\frac{p_T^2}{m_H^2}$ .

For this study  $\frac{m_H^2}{s} = 10^{-1}$  was chosen and two quark masses were tested. The plots for the quark mass  $(2m_q/m_H)^2 = 10^{-2}$  are shown in figures 3a to 5b and for the smaller

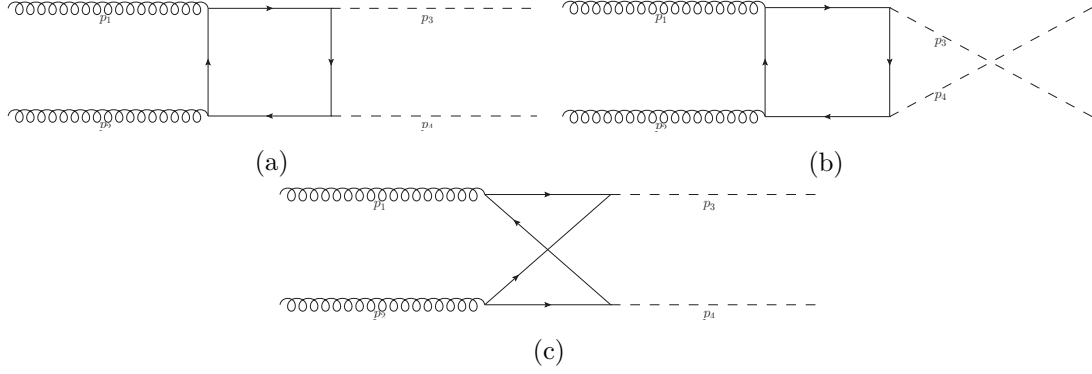


Figure 2: a and b: straight box diagrams; c: crossed box diagram

quark mass  $(2m_q/m_H)^2 = 10^{-4}$  are shown in figures 6a to 8b. The scale  $4m_q^2/m_H^2$  was chosen, because many variables and the amplitude itself depends mostly on  $4m_q^2$ , not only on the factor  $m_q^2$ .  $4m_q^2$  can be understood as the invariant mass of two quarks after the splitting of a gluon and therefore sets the important scale of this problem.

One can see that the evaluation at  $p_T = 0$  is not possible numerically. However it is possible to go as close to this as desired without numerical problems. First, the end of the plots at low  $p_T$  is due to the spacing chosen in  $p_T$ . Second, ever 3- and 4-point function saturates for small  $p_T$  and a linear interpolation is possible.

Because the 3- and 4-point functions do not have numerical problems,  $gauge_1$  is also well behaved. There is only one term in the amplitude  $gauge_2$  that is proportional to  $1/p_T^2$  and can therefore impose problems. For the numerical evaluation factors of  $m_q^2$ , which correspond to the higgs coupling to the quarks in the loop, have been normalized to unity. To study the numerical stability  $gauge_2$  is divided in an regular term

$$gauge_{2,reg} = 4(8m_q^2 + s - 2m_H^2)(m_q^2[D(p_1, p_2, p_3) + D(p_2, p_1, p_3) + D(p_1, p_3, p_2)] - C(p_3, p_4)) - 4[sC(p_1, p_2) + (t - m_H^2)C(p_1, p_3) + (u - m_H^2)C(p_2, p_3)] \quad (4.1)$$

and an irregular term

$$gauge_{2,ireg} = \frac{2}{p_T^2} \left( su(8um_q^2 - u^2 - m_H^4)D(p_1, p_2, p_3) + st(8tm_q^2 - t^2 - m_H^4)D(p_2, p_1, p_3) + (8m_q^2 + s - 2m_H^2)(s(s - 2m_H^2)C(p_1, p_2) + s(s - 4m_H^2)C(p_3, p_4) + 2t(m_H^2 - t)C(p_1, p_3) + 2u(m_H^2 - u)C(p_2, p_3)) \right). \quad (4.2)$$

As one can see in figures 5b and 8b  $gauge_{2,ireg}$  shows oscillating behaviour for

$$\frac{p_T^2}{m_H^2} < 10^{-4} \text{ (large quark mass) and } \frac{p_T^2}{m_H^2} < 10^{-3} \text{ (small quark mass)}$$



because of the division through  $p_T^2$ .

But also in this case it is possible to get close enough to small  $p_T$  values to see the saturating effect and extrapolate the behaviour. In section 4.2 it is also shown that this part of  $gauge_2$  can also be well approximated for small quark masses.

Thus numerical stability is under good control for the evaluation of these amplitudes.

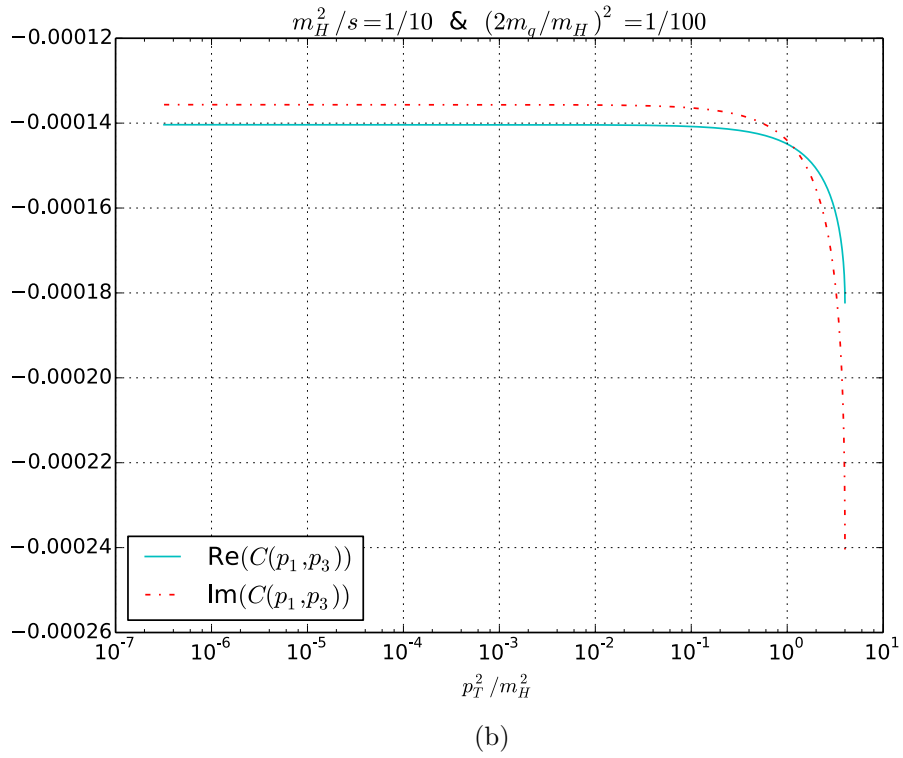
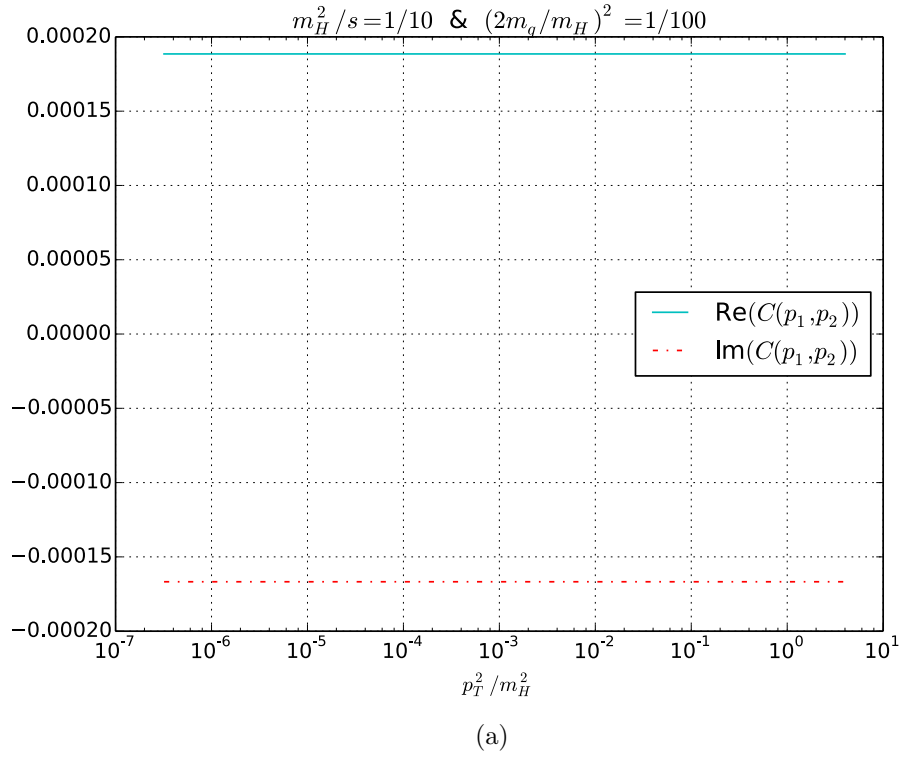


Figure 3:  $C(p_1, p_2)$  and  $C(p_1, p_3)$  for the larger quark mass

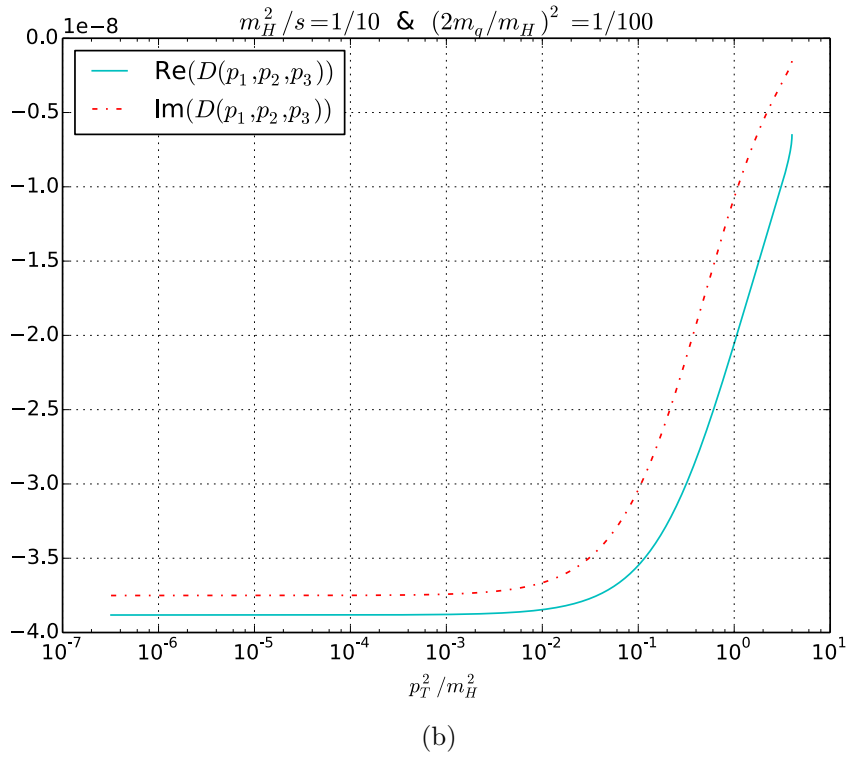
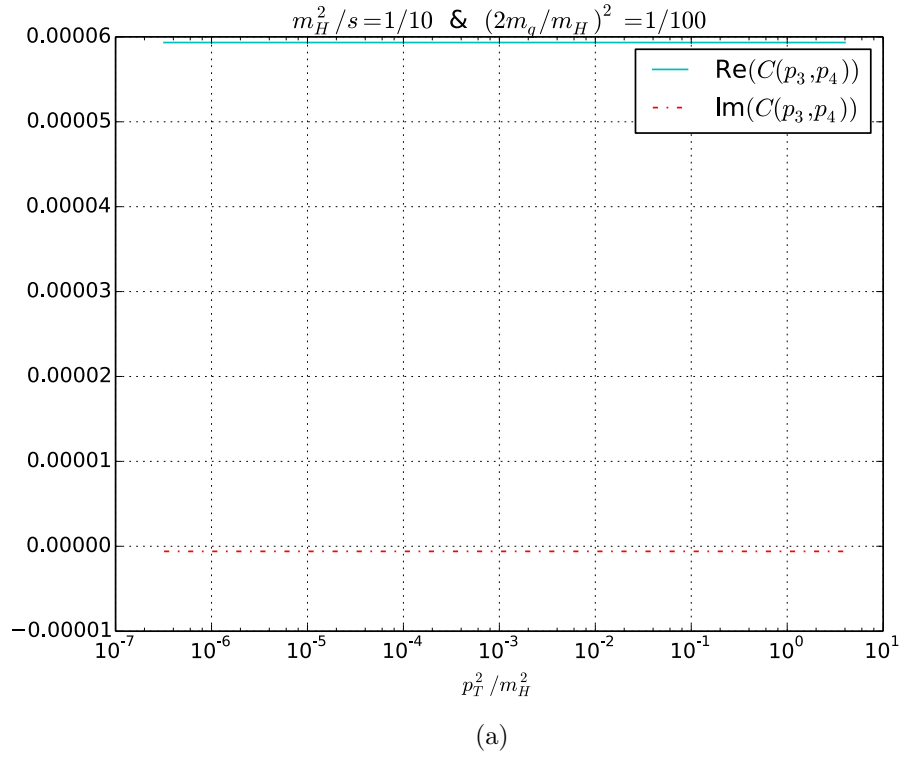


Figure 4:  $C(p_3, p_4)$  and  $D(p_1, p_2, p_3)$  for the larger quark mass

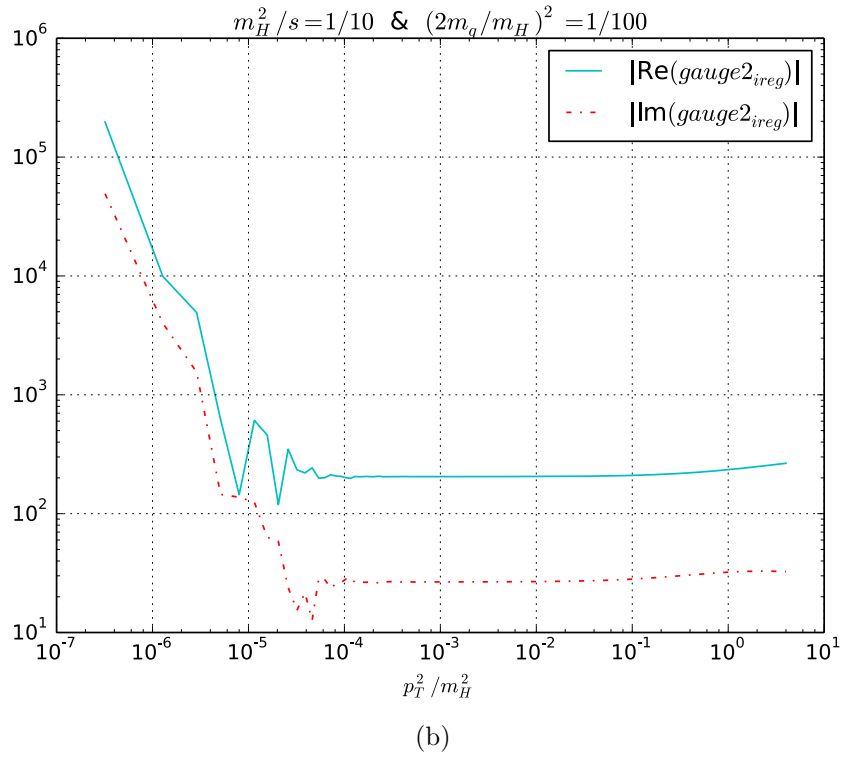
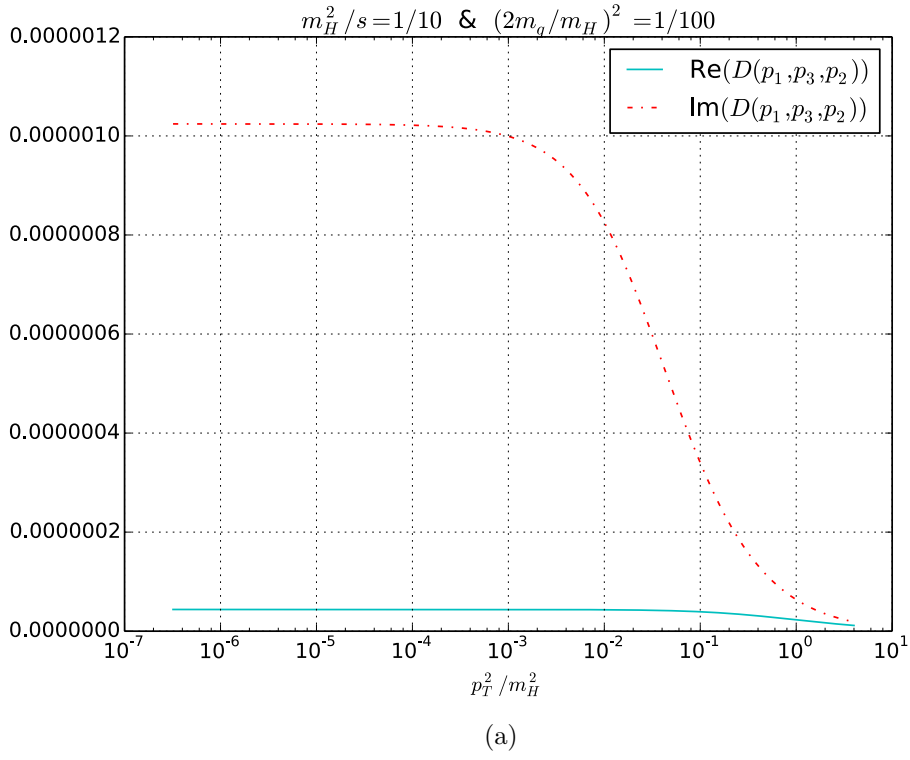


Figure 5:  $D(p_1, p_2, p_3)$  and  $gauge_{1,ireg}$  for the larger quark mass

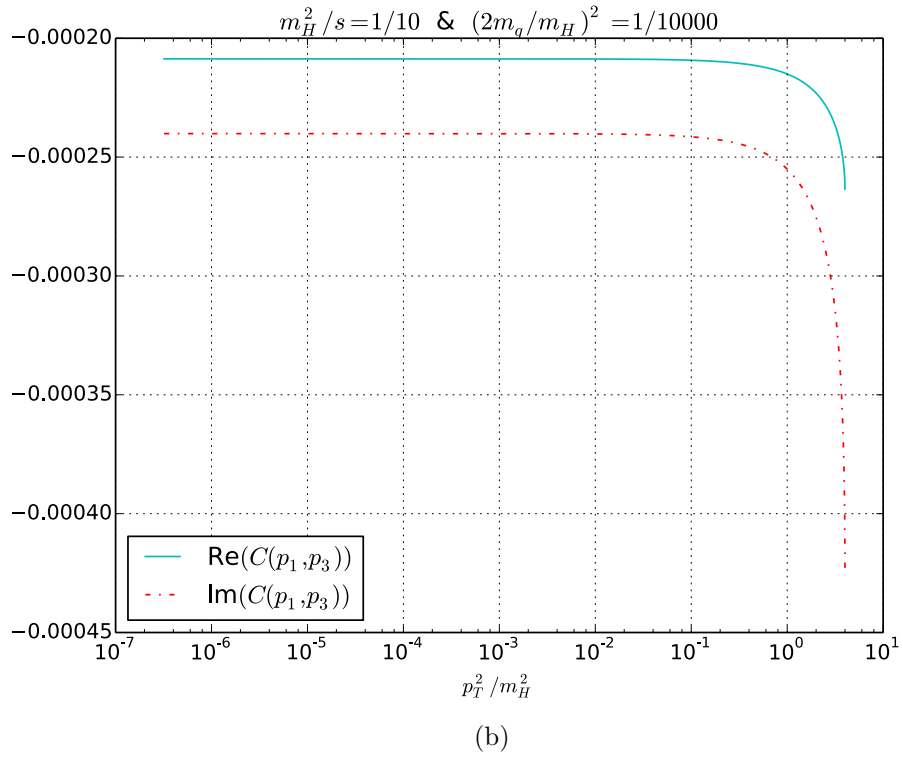
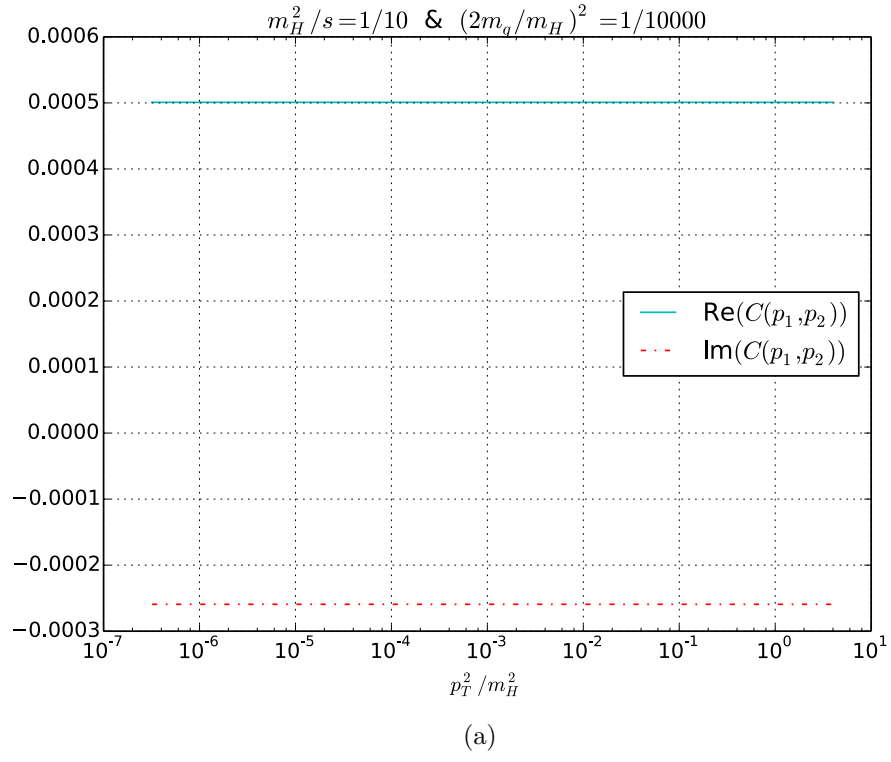


Figure 6:  $C(p_1, p_2)$  and  $C(p_1, p_3)$  for the smaller quark mass

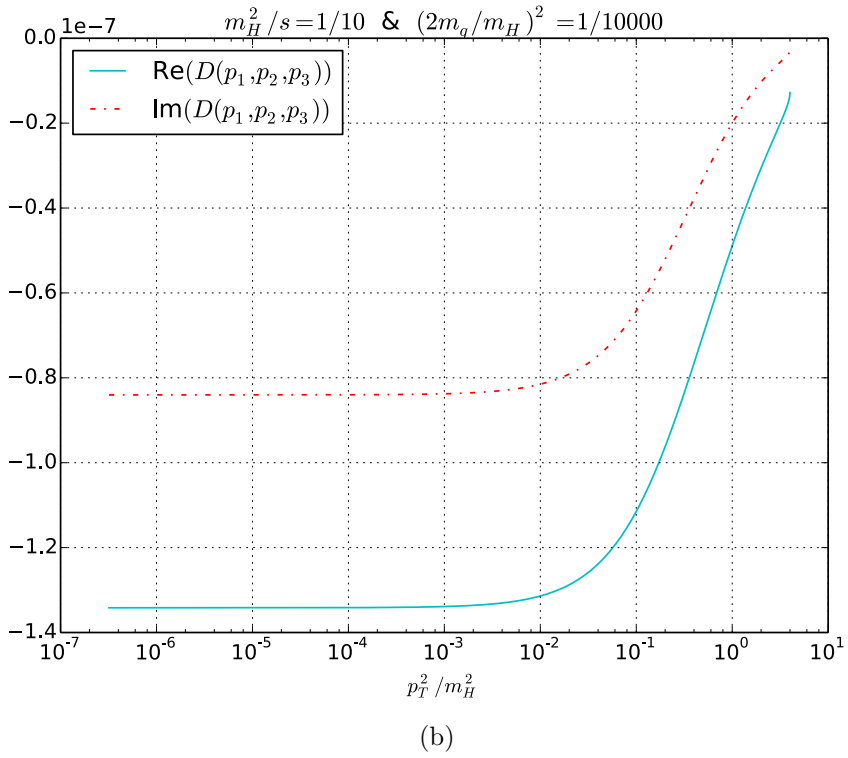
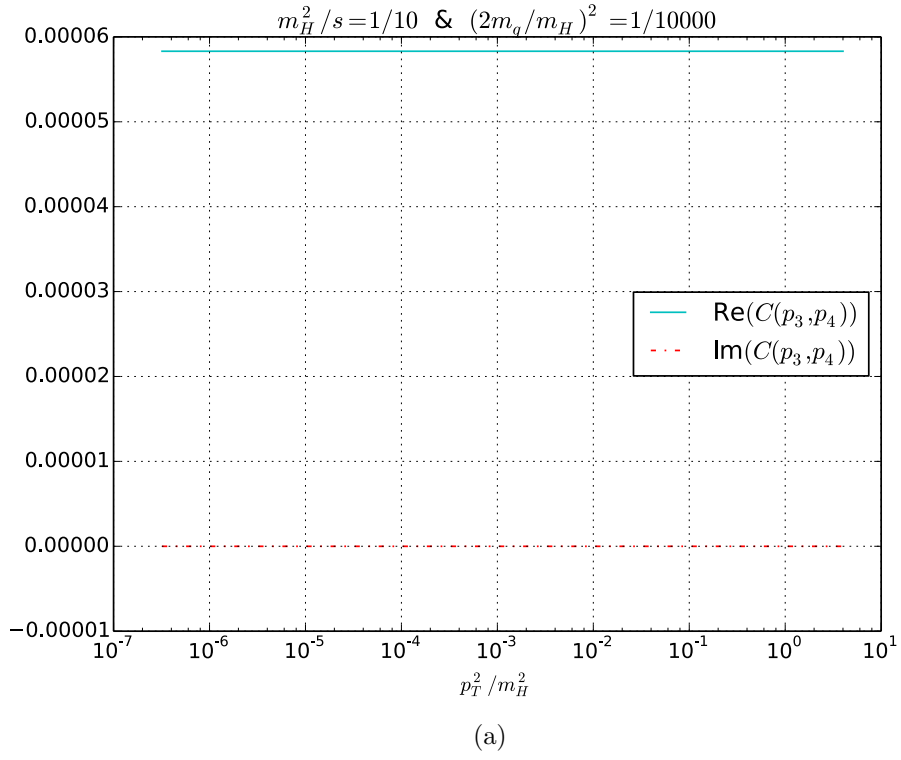


Figure 7:  $C(p_3, p_4)$  and  $D(p_1, p_2, p_3)$  for the smaller quark mass

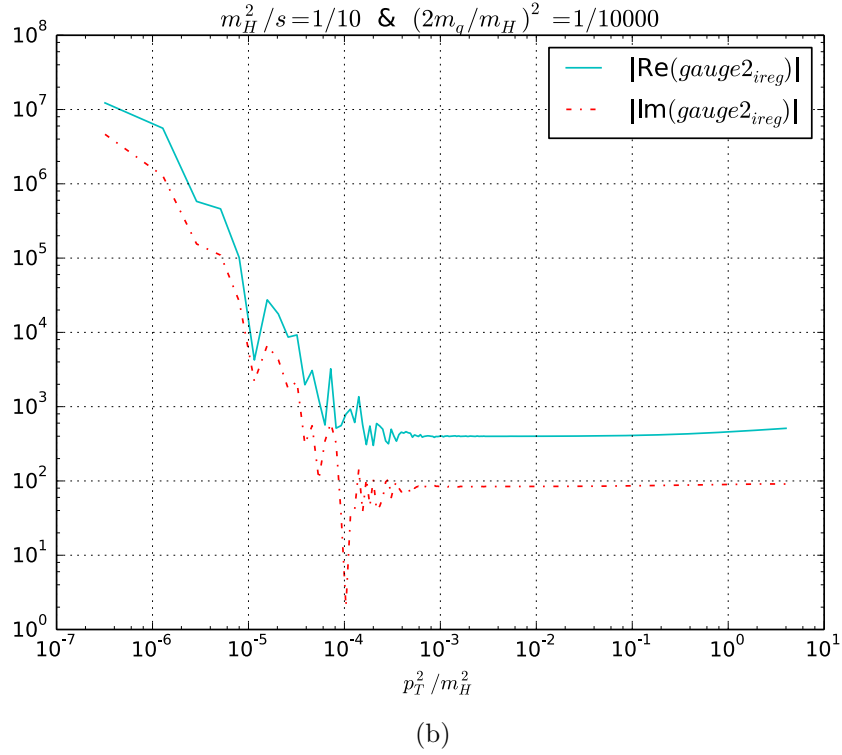
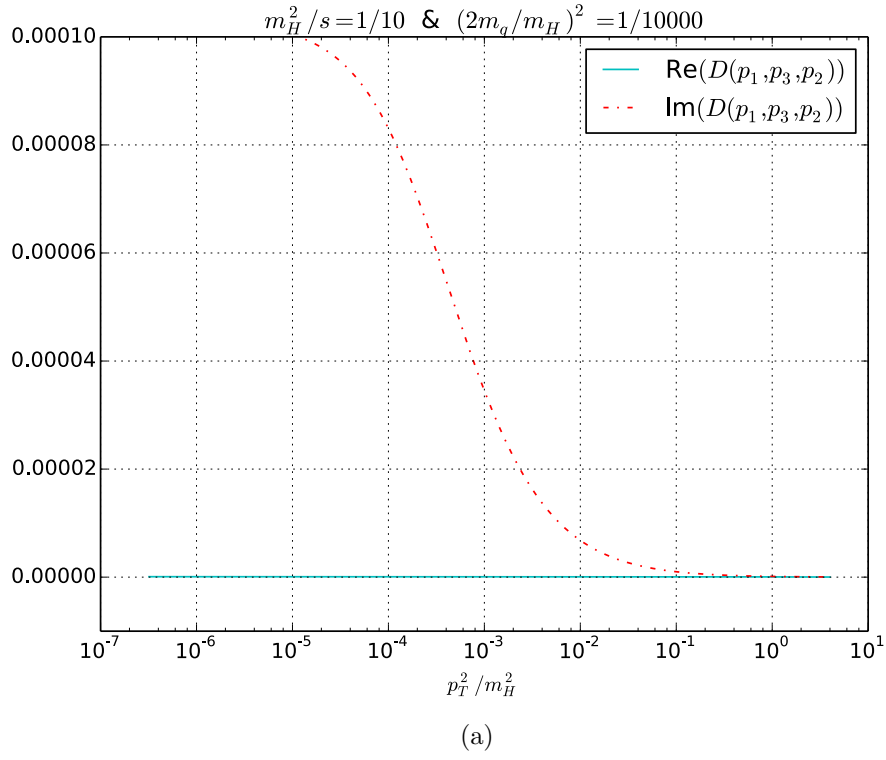


Figure 8:  $D(p_1, p_3, p_2)$  and  $gauge_{2,ireg}$  for the smaller quark mass

## 4.2. Cross Check with $m_q$ -Expansion

In this section the implementation of the amplitude is compared with the low  $m_q$ -expansion found in [4]. Because in section 3.3 it was shown that the expansions in  $m_q$  and  $p_T$  do not commute for the crossed box diagram  $D(p_1, p_3, p_2)$ , the parts of  $gauge_1$  with contributions from the crossed box are studied separately. For this purpose

$$\begin{aligned} gauge_{1,good} = & 4m_q^2 (8m_q^2 - s - 2m_H^2) (D(p_1, p_2, p_3) + D(p_2, p_1, p_3)) \\ & + 8 + 16m_q^2 C(p_1, p_2) \\ & + \frac{8}{s} (m_H^2 - 4m_q^2) [(t - m_H^2) C(p_1, p_3) + (u - m_H^2) C(p_2, p_3)] \end{aligned} \quad (4.3)$$

and

$$\begin{aligned} gauge_{1,bad} = & 4m_q^2 (8m_q^2 - s - 2m_H^2) D(p_1, p_3, p_2) \\ & + \frac{ut - m_H^4}{s} (4m_q^2 - m_H^2) D(p_1, p_3, p_2) \end{aligned} \quad (4.4)$$

are introduced. The results for two different quark masses are shown in figures 9 to 16.  $Gauge_2$  is split up in his regular and irregular part, because of numerical stability and because only the irregular part contains contributions from the crossed box.

One can see that the  $m_q$ -expansion does yield to good results for  $gauge_{1,good}$ ,  $gauge_{2,ireg}$  and the real parts of  $gauge_{1,bad}$  and  $gauge_{2,reg}$ , only the imaginary part of the crossed box is approximated poorly which leads to seizable deviations in the imaginary parts of  $gauge_{1,bad}$  and  $gauge_{2,reg}$ . This can be explained by the not commuting of the limits shown in 3.3. Because the crossed box only appears with a factor of  $m_q^2$  the implications on the real part are negligible, but the term proportional to  $\frac{1}{m_q^4}$  and  $\frac{1}{m_q^2}$  leads to seizable deviations even multiplied by  $m_q^2$ .

Another feature of the  $m_q$ -expansion is the fact that the amplitudes  $gauge_1$  and  $gauge_2$  do not depend on  $m_q$  any more. This was also tested by comparing the amplitudes at the small quark mass versus  $m_q$  set to  $s$ . The deviations were of the order  $10^{-9}$  and therefore negligible, verifying this property.

Also the imaginary part of  $gauge_1$  in the small  $m_q$ -limit should be dominated by the logarithmic divergence in the transverse momentum, corresponding to the double parton singularity. This can be seen in figure 17, where the exact, the  $m_q$ -limit and the leading term in the  $m_q$ -limit for the imaginary part of  $gauge_1$  are plotted. One can see that over a large range of  $p_T$  the leading term describes the  $m_q$ -limit very well.



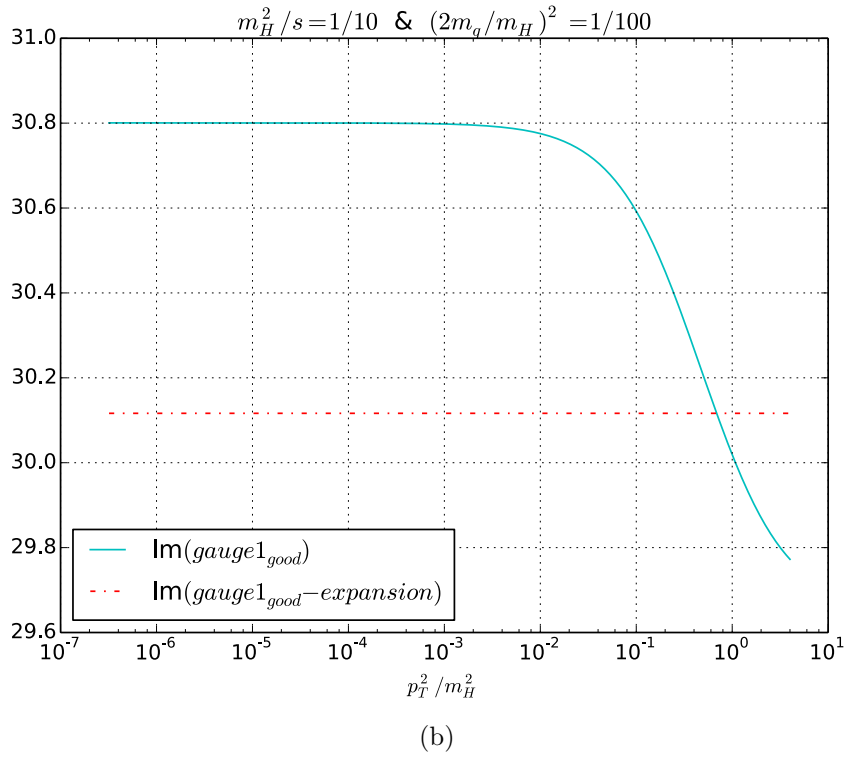
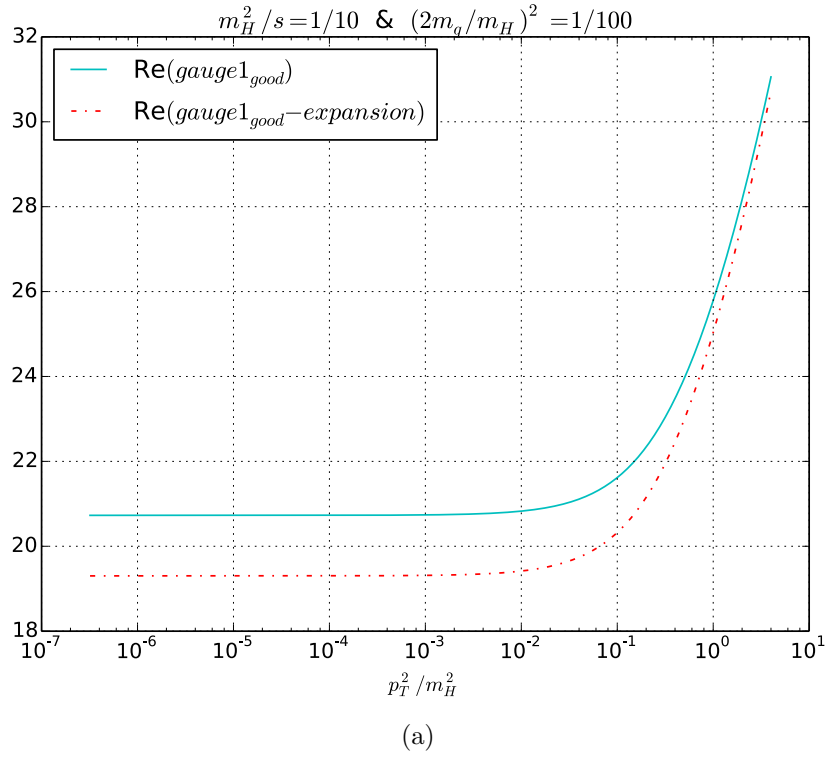


Figure 9: Real and imaginary part of  $gauge_{1,good}$  for the larger quark mass

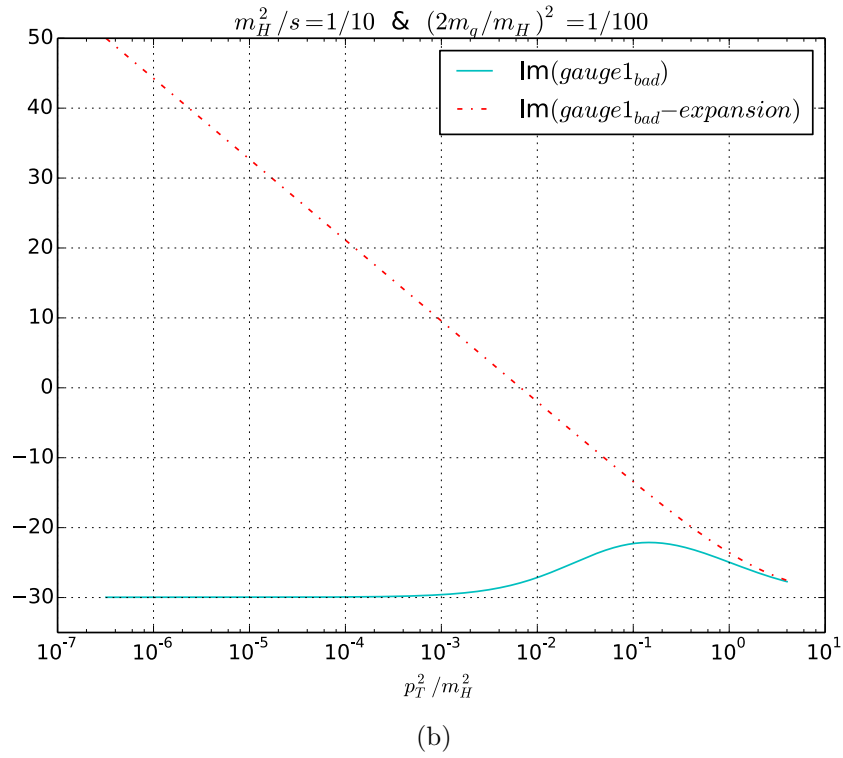
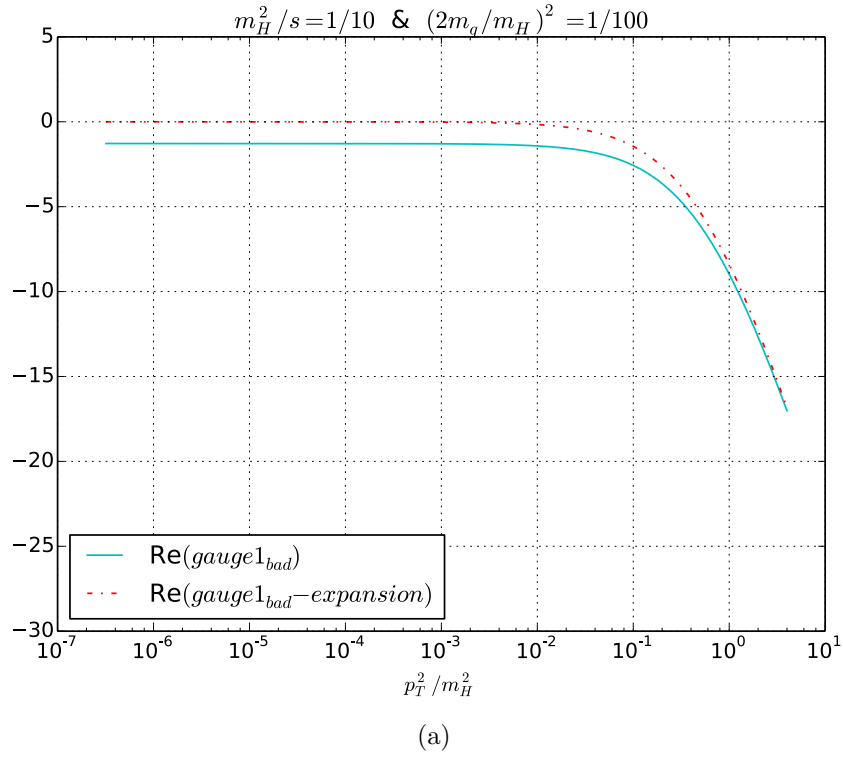


Figure 10: Real and imaginary part of  $gauge_{1,bad}$  for the larger quark mass

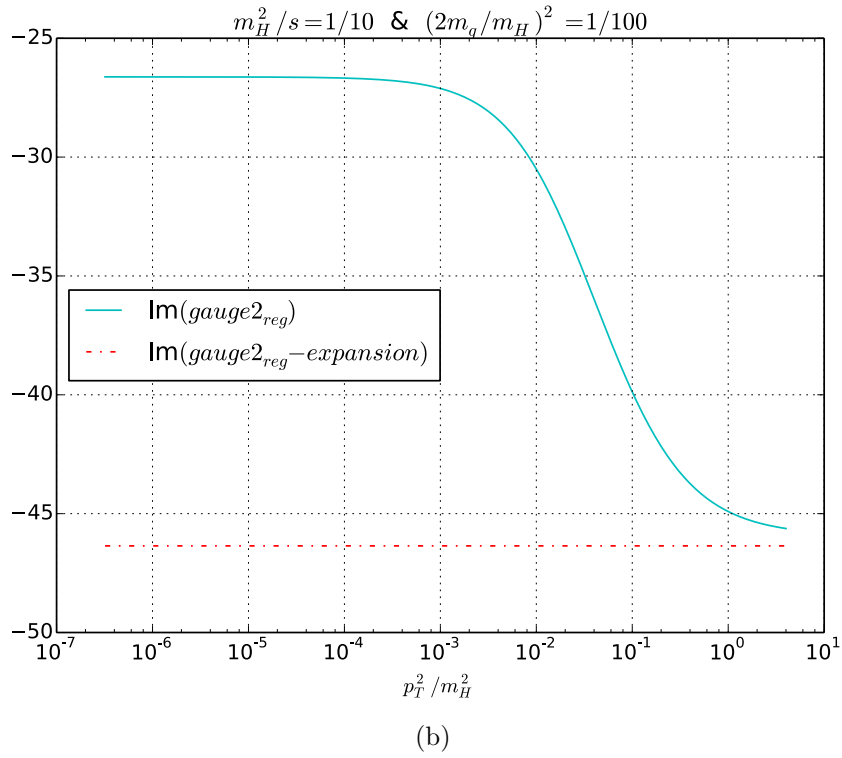
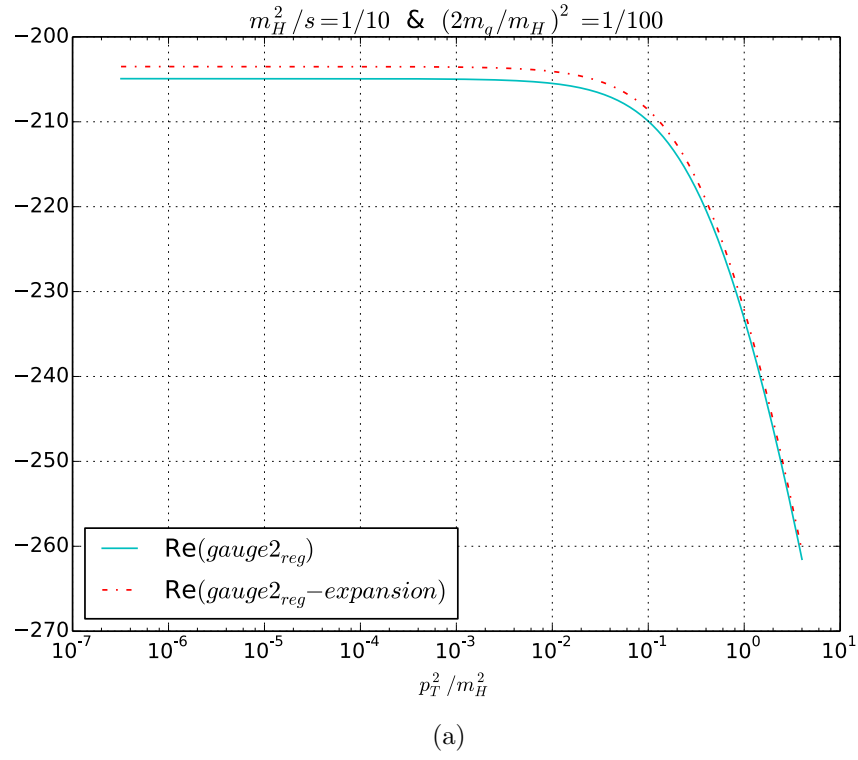


Figure 11: Real and imaginary part of  $gauge_{2,reg}$  for the larger quark mass

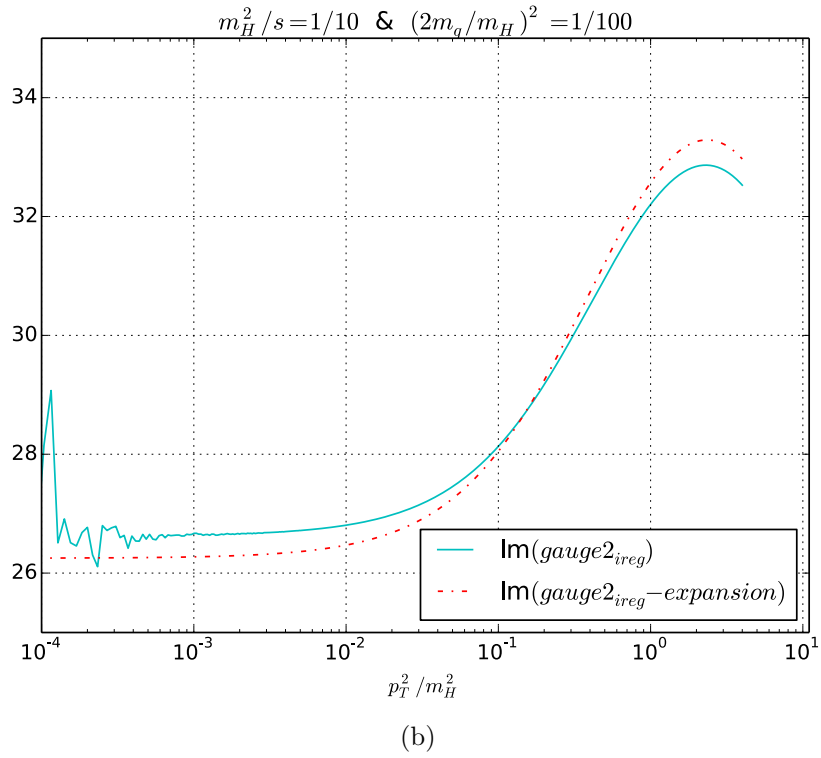
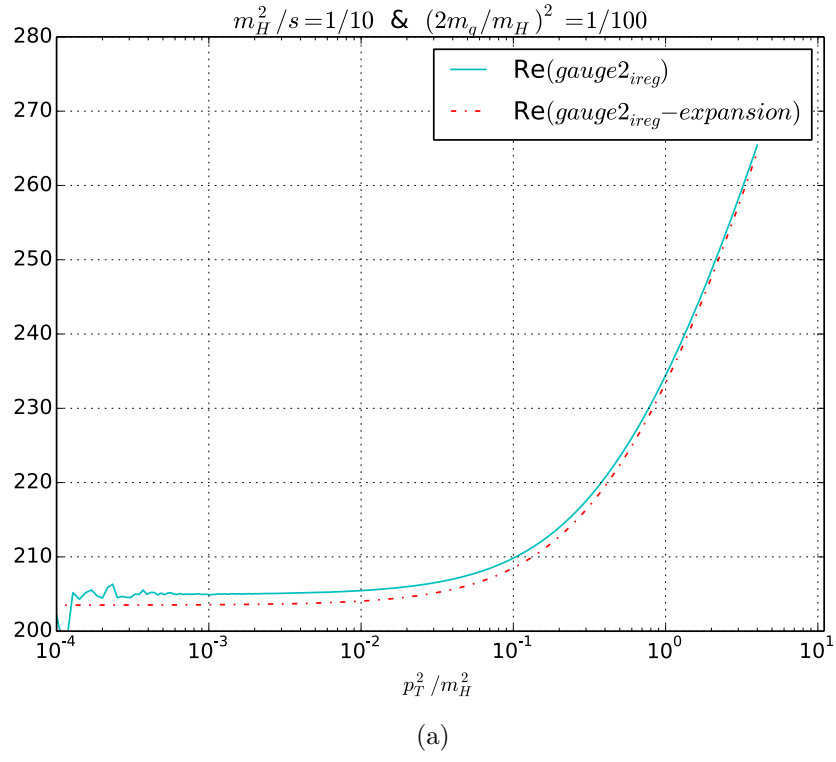


Figure 12: Real and imaginary part of  $gauge_{2,ireg}$  for the larger quark mass

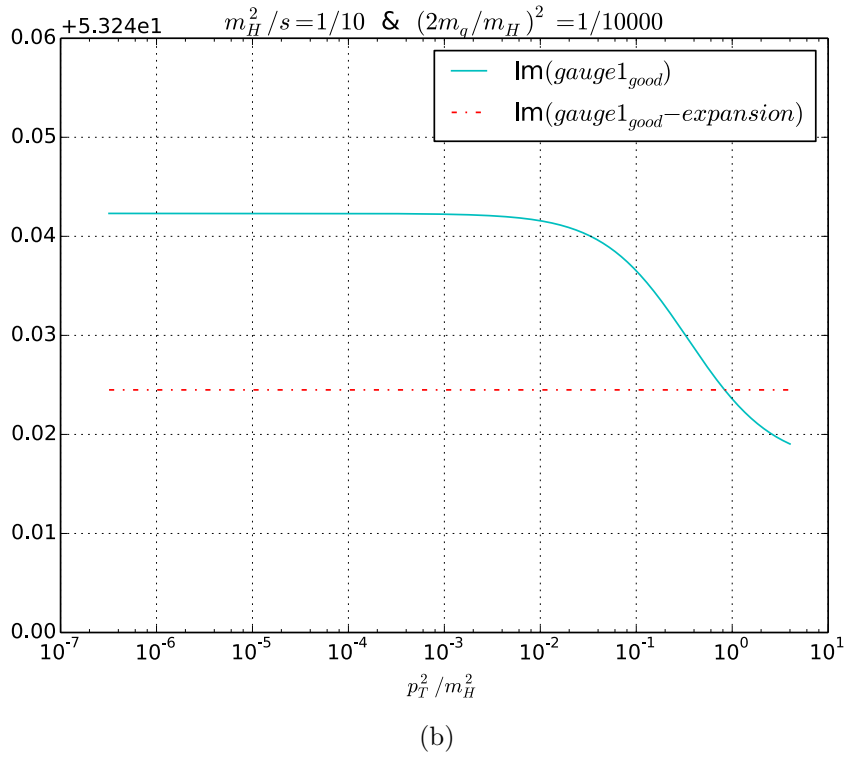
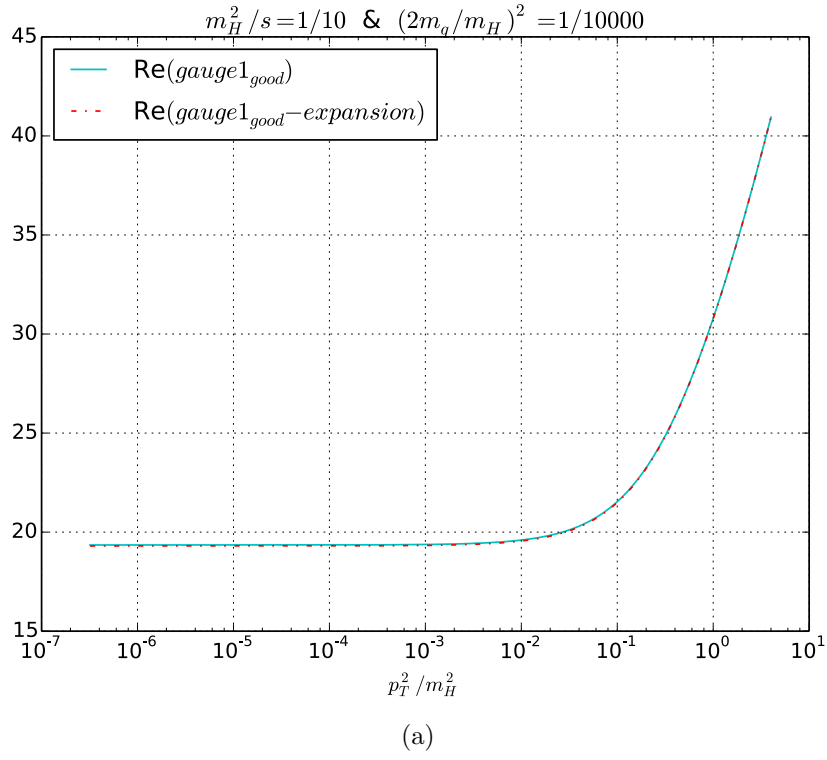


Figure 13: Real and imaginary part of  $gauge_{1,good}$  for the smaller quark mass

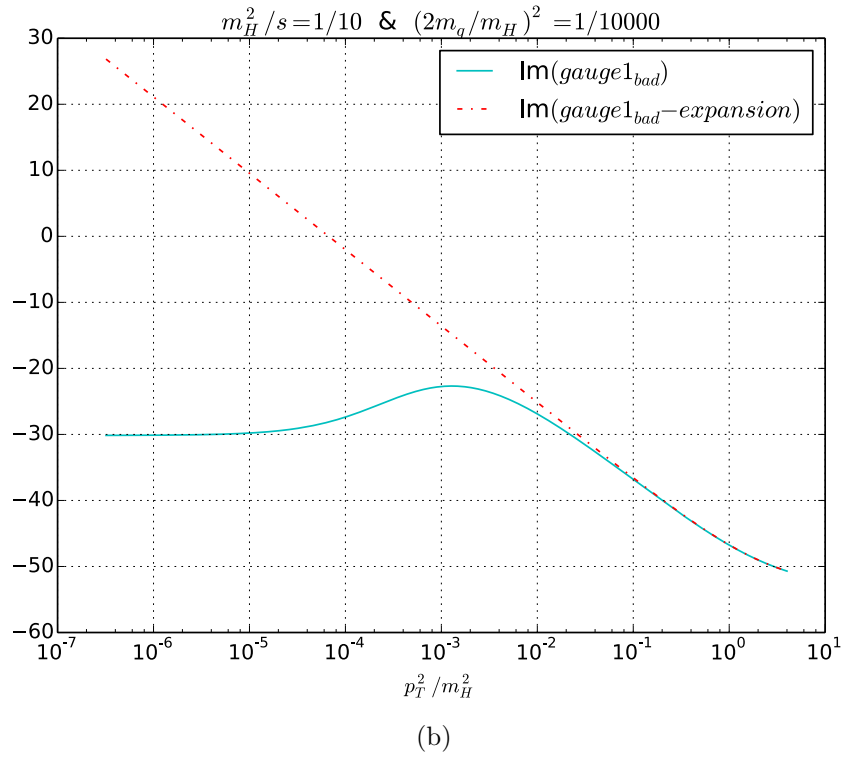
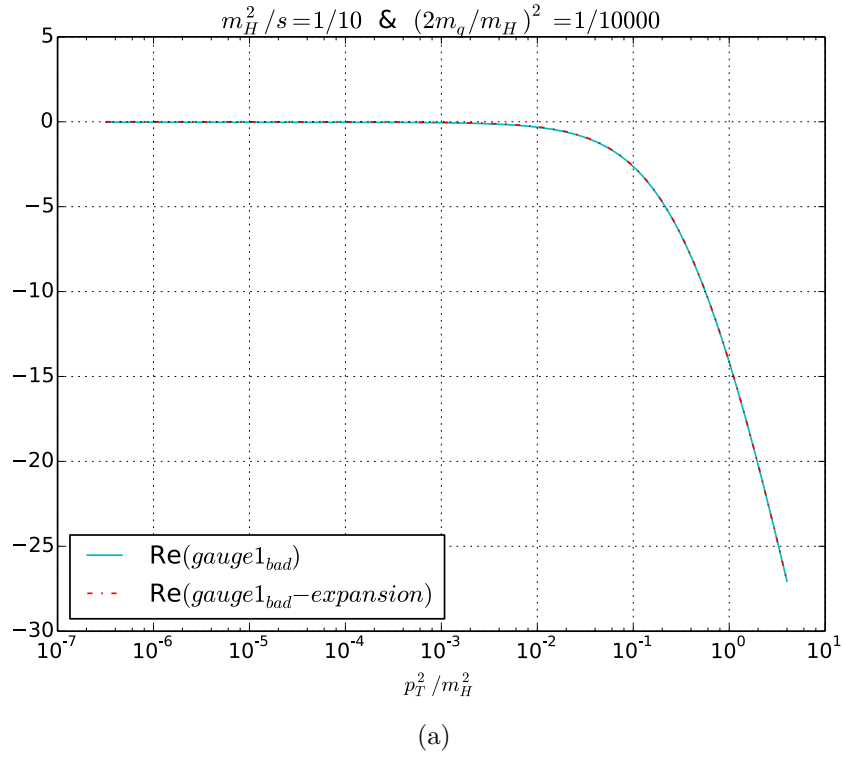


Figure 14: Real and imaginary part of  $gauge_{1,bad}$  for the smaller quark mass

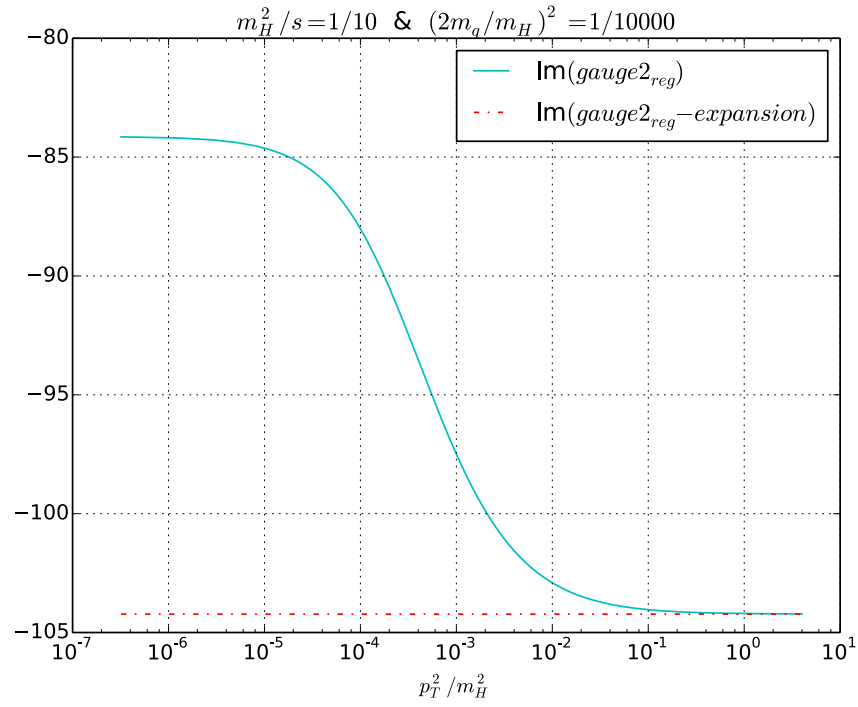
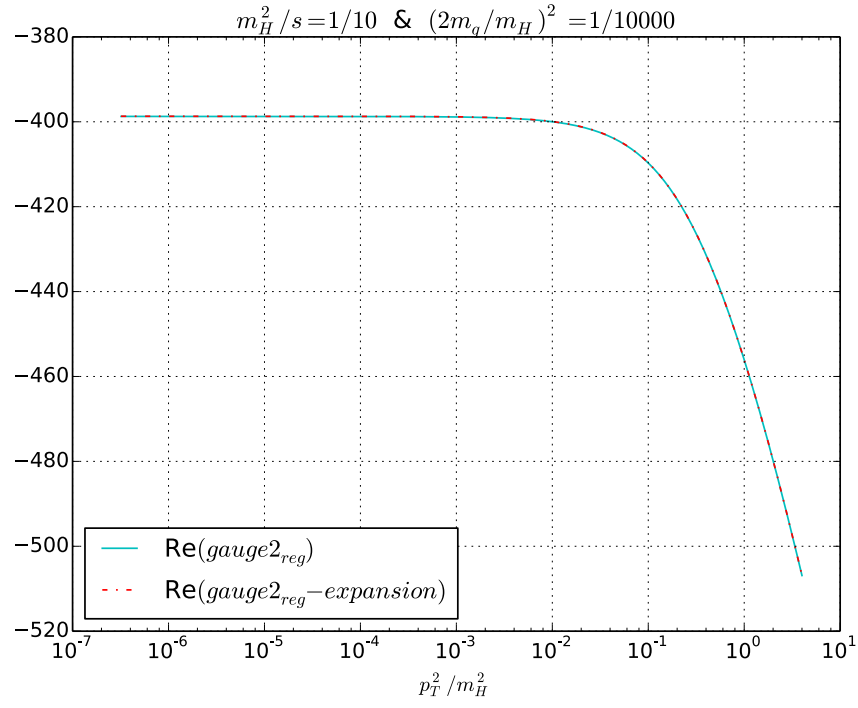


Figure 15: Real and imaginary part of  $gauge_{2,reg}$  for the smaller quark mass

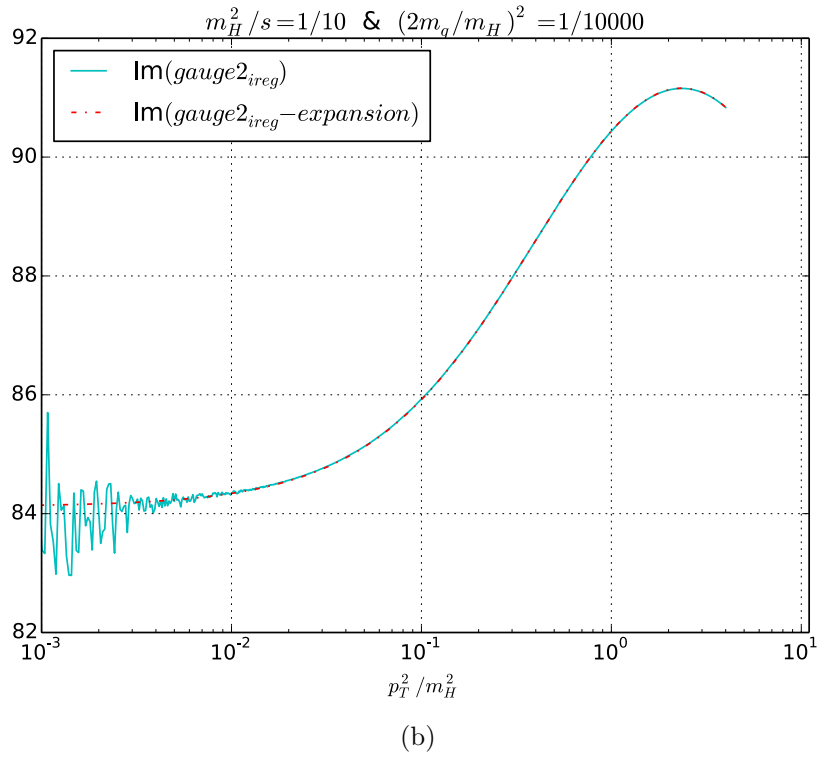
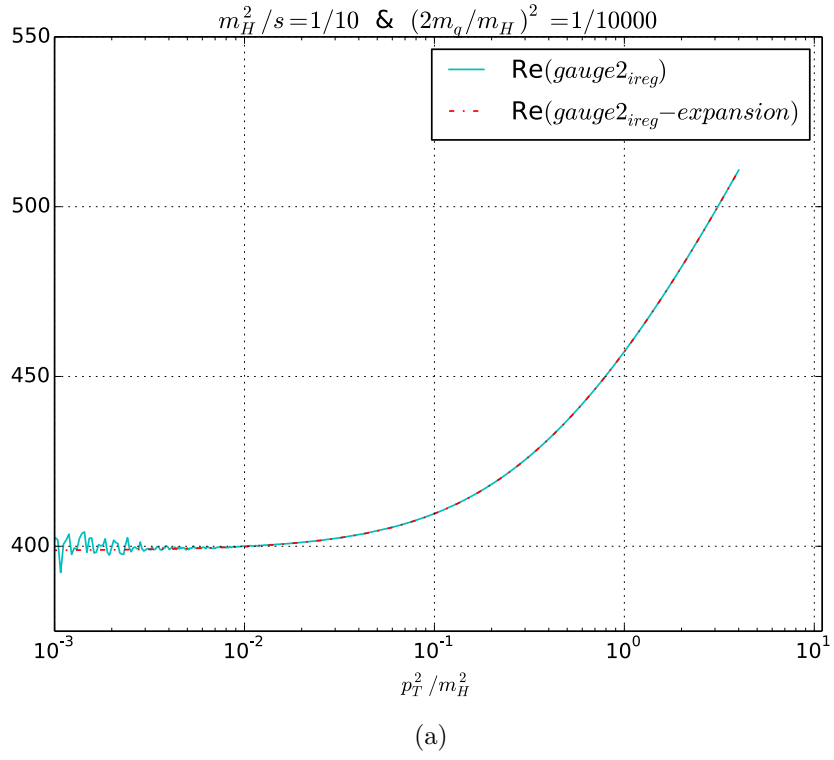


Figure 16: Real and imaginary part of  $gauge_{2,ireg}$  for the smaller quark mass



### 4.3. Cross Check with $p_T$ -Expansion

To show the validity of the  $p_T$ -series for the crossed box given in 3.3 the exact result, the  $m_q$ -series and the  $p_T$ -series are shown for the larger quark mass in figure 18a and for smaller quark mass in figure 18b. One can see that the  $p_T$ -series gets better with higher quark masses and describes the crossed box very well in the region where the  $m_q$ -series cannot describe the exact result.

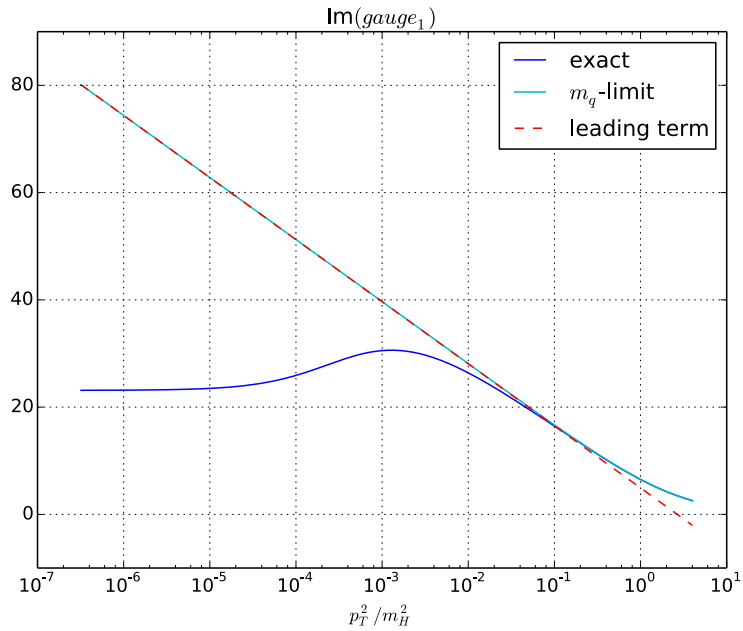


Figure 17: Exact,  $m_q$ -limits and leading term of  $\text{Im}(gauge_1)$

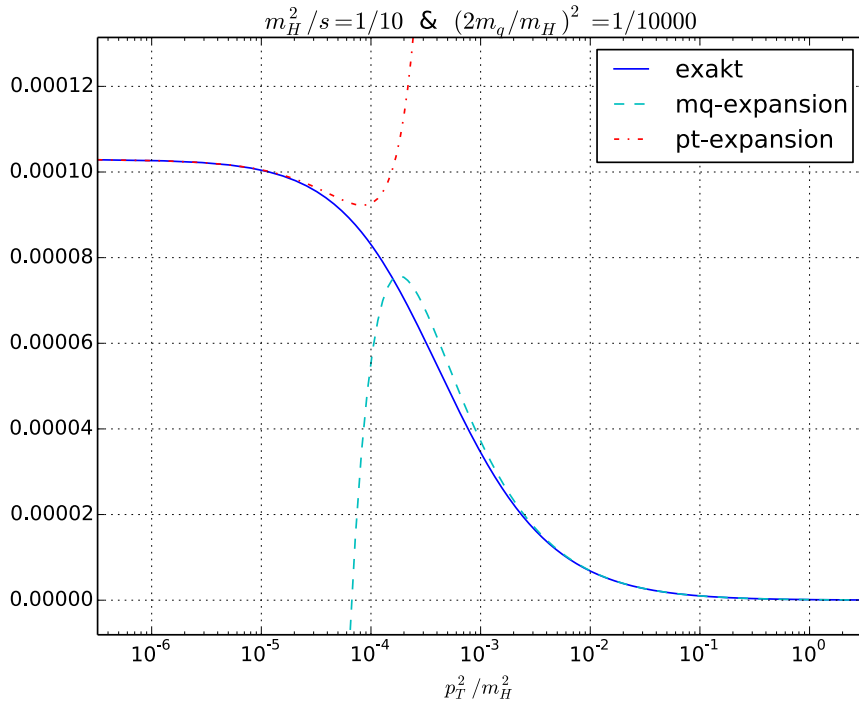
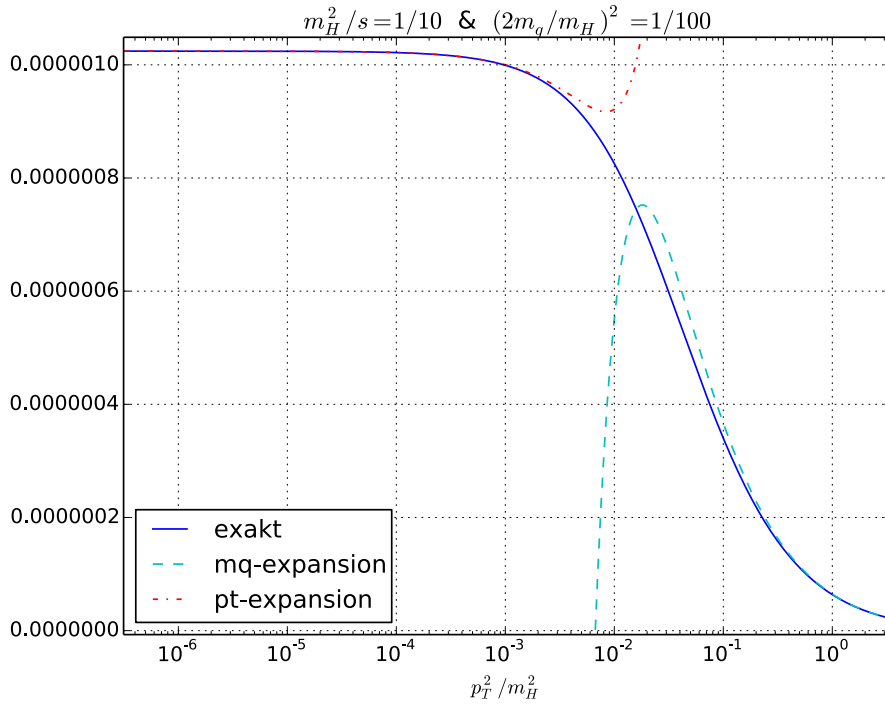


Figure 18: Exact results, leading terms of the  $m_q$ -series and the  $p_T$ -series for the crossed box diagram

#### 4.4. Results

After getting a better analytical understanding and validating the numerical result for the amplitude, the quark mass dependence of the cross section is analysed by evaluating

$$|gauge_1|^2 + |gauge_2|^2 ,$$

which is proportional to the differential cross section [5]. To avoid the numerical instability of  $gauge_{2,ireg}$  the  $m_q$ -series was used for this term, which only leads to small deviations shown in 4.2. The results are shown in figure 19.

The maximum cross section is always at  $p_T \neq 0$  and is shifted to higher values of  $p_T$  as  $m_q$  grows. However the cross section for small transverse momentum increases with decreasing  $m_q$ , which is natural, because one expects a collinear, logarithmic divergence at  $p_T = m_q = 0$ . This can also be seen in the linear dependence after the maximum. The quark mass regulates therefore the logarithmic divergence.

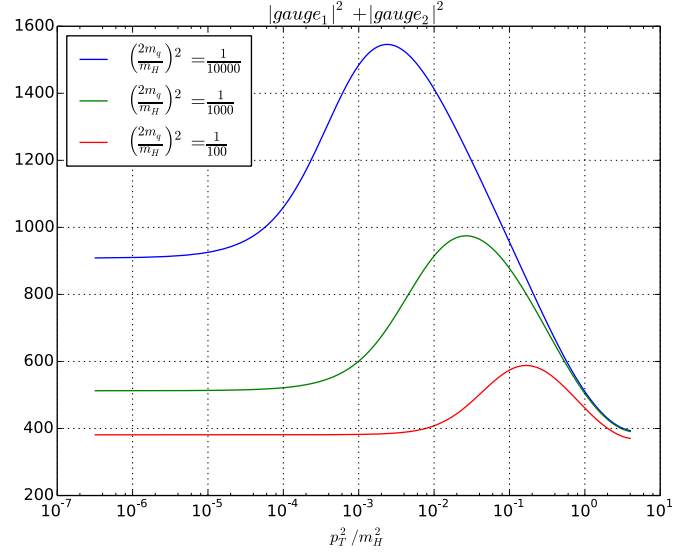


Figure 19:  $|gauge_1|^2 + |gauge_2|^2$  for different quark masses

## 5. Conclusion

It was shown that the imaginary part of every 3- and 4-point function can be extracted analytically for higgs boson pair production via gluon fusion. Furthermore it was shown that the limits for small quark masses and small transverse momentum do not commute for the crossed box and that one has to be very careful what approximations can be made in the kinematic region. Also the code implemented to compute the amplitudes was cross checked with both limits, providing a good verification.

The next step is to integrate the squared amplitude over phase space to get the total cross section of this process.

In a further study this functions can also be used to evaluate Z boson pair production via gluon fusion described in [4], which helicity amplitudes depend on the same 3- and 4- point functions.

## A. Kinematic Variables

$$\alpha = 1 - \frac{s}{2m_H^2} \left( 1 + \sqrt{1 - \frac{4m_H^2}{s}} \right), \quad (\text{A.1})$$

$$y_0 = \frac{\alpha}{\alpha + 1}, \quad y'_0 = \frac{\alpha^2}{\alpha^2 - 1} \quad (\text{A.2})$$

$$x_{\pm} = \frac{1}{2} \left( 1 \pm \frac{\sqrt{p_T^2 + 4m_q^2}}{p_T} \right), \quad p_T^2 = \frac{ut - m_H^4}{s} \quad (\text{A.3})$$

$$\beta_1 = -\frac{u}{m_H^2 - u}, \quad v = -\sqrt{1 - \frac{4m_H^2}{s}}, \quad (\text{A.4})$$

$$\beta_2 = \frac{1}{2} (1 + v) \quad Y = -su \sqrt{1 + \frac{4m_q^2 p_T^2}{u^2}}, \quad (\text{A.5})$$

$$y_{1\pm} = \frac{-u \pm \frac{Y}{s}}{2(u - m_H^2)}, \quad y_{2\pm} = \frac{-m_H^2 + m_H^2 v - uv \pm \frac{Y}{s}}{2u - 2m_H^2 + s - sv} \quad (\text{A.6})$$

## B. Evaluation of the Imaginary Part

To check if

$$I_1(a, b, y_0) = \underbrace{\text{Li}_2 \left( \frac{y_0}{y_0 - z} \right)}_{=(i)} - \underbrace{\text{Li}_2 \left( \frac{y_0 - 1}{y_0 - z} \right)}_{=(ii)}, \quad (\text{B.1})$$

with  $z = -\frac{b-i\varepsilon}{a}$  has a non vanishing imaginary part, one has to check if the real part of the argument is bigger than one. To do so the following information on the kinematic variables are necessary

$$u = -\frac{s}{2} (1 - v \cos(\theta)) + m_H^2 < -m_H^2 \quad (\text{B.2})$$

$$t = -\frac{s}{2} (1 + v \cos(\theta)) + m_H^2 < -m_H^2 \quad (\text{B.3})$$

$$p_T^2 = \frac{ut - m_H^4}{s} = \left( \frac{s}{4} - m_H^2 \right) (1 - \cos^2(\theta)) \in \left[ 0, \frac{s}{4} - m_H^2 \right] \quad (\text{B.4})$$

$$\frac{\alpha}{\alpha + 1} < -1 \quad (\text{B.5})$$

$$\frac{\alpha^2}{\alpha^2 - 1} > 1 \quad (\text{B.6})$$

$$\frac{Y}{s} = -u \sqrt{1 + 4m_q^2 \frac{p_T^2}{u^2}} = -u \left( 1 + 2m_q^2 \frac{p_T^2}{u^2} \right) = -u + \delta \quad (\text{B.7})$$

in leading order in  $m_q^2$ . Moreover

$$\frac{y_{1+}}{1-\beta_1} = \frac{u - \frac{Y}{s}}{2m_H^2} = \frac{u}{m_H^2} + \frac{\delta}{2m_H^2} < 0 \quad (\text{B.8})$$

$$\frac{y_{1-}}{1-\beta_1} = \frac{u + \frac{Y}{s}}{2m_H^2} = \frac{\delta}{2m_H^2} > 0 \quad (\text{B.9})$$

$$\frac{m_H^2 - u}{m_H^2 - t} = \frac{1 - v \cos(\theta)}{1 + v \cos(\theta)} = \frac{s}{4m_H^2} (1 - v \cos(\theta))^2 > \frac{s}{4m_H^2} (1 + v)^2 = -1 + \frac{s}{2m_H^2} (1 + v) \quad (\text{B.10})$$

$$\frac{y_{1+}}{\beta_1} = \frac{-u + \frac{Y}{s}}{2u} = -1 + \frac{\delta}{2u} < -1 \quad (\text{B.11})$$

$$\frac{y_{1-}}{\beta_1} = \frac{-u - \frac{Y}{s}}{2u} = \frac{-\delta}{2u} > 0 \quad (\text{B.12})$$

$$\beta_2 + y_{2+} = \frac{2m_H^2 + \delta}{-sv(1+x)} > 0 \quad (\text{B.13})$$

$$\beta_2 + y_{2-} = \frac{2u + 2m_H^2 - \delta}{-sv(1+x)} < 0 \quad (\text{B.14})$$

$$\frac{y_{2+}}{1-\beta_2} = \frac{s(1-v) - 4m_H^2 + \delta}{sv(v-1)} = 1 + \frac{\delta}{sv(v-1)} > 1 \quad (\text{B.15})$$

$$\frac{y_{2-}}{1-\beta_2} = \frac{-2m_H^2 - \delta}{sv(v-1)} < 0 \quad (\text{B.16})$$

$$\frac{y_{2+}}{\beta_2} = -1 - \frac{\delta}{(-s - sv + 4m_H^2)(x+1)} < -1 \quad (\text{B.17})$$

$$\frac{y_{2-}}{\beta_2} = \frac{(1-v)(x-1)s - 4xm_H^2}{(x+1)(-(1+v)s + 4m_H^2)} > 0 \quad (\text{B.18})$$

$$\frac{p_T^2}{u} + 1 = \frac{u(t+s) - m_H^4}{su} = \frac{-\frac{s}{4}(1+vx)^2}{su} > 0. \quad (\text{B.19})$$

With this information it is possible to extract if a dilogarithm gets an imaginary part, the results are shown in table 1.

The results for the

$$I_2(a, b, y_0) = \underbrace{\text{Li}_2\left(\frac{y_0}{y_0 - z_1}\right)}_{=(I)} - \underbrace{\text{Li}_2\left(\frac{y_0 - 1}{y_0 - z_1}\right)}_{=(II)} + \underbrace{\text{Li}_2\left(\frac{y_0}{y_0 - z_2}\right)}_{=(III)} - \underbrace{\text{Li}_2\left(\frac{y_0 - 1}{y_0 - z_2}\right)}_{=(IV)} \quad (\text{B.20})$$

functions, with  $z_1 = \frac{1}{2} \left(1 + \sqrt{1 - 4\frac{a-i\varepsilon}{b}}\right)$  and  $z_2 = 1 - z_1$  are given in table 2.

	(i)	(ii)
$I_1(s, 0, \beta_1 + y_{1+})$	$\times$	$\checkmark$
$I_1(s, 0, \beta_1 + y_{1-})$	$\times$	$\times$
$I_1(m_H^2 - t, m_H^2 - u, y_{1+}/(1 - \beta_1))$	$\checkmark$	$\checkmark$
$I_1(m_H^2 - t, m_H^2 - u, y_{1-}/(1 - \beta_1))$	$\times$	$\times$
$I_1(u - m_H^2, m_H^2 - u, -y_{1+}/\beta_1)$	$\checkmark$	$\times$
$I_1(u - m_H^2, m_H^2 - u, -y_{1-}/\beta_1)$	$\times$	$\times$
$I_1(s, 0, \beta_2 + y_{2+})$	$\times$	$\times$
$I_1(s, 0, \beta_2 + y_{2-})$	$\times$	$\checkmark$
$I_1(m_H^2 - t, m_H^2 - u, y_{2+}/(1 - \beta_2))$	$\times$	$\times$
$I_1(m_H^2 - t, m_H^2 - u, y_{2-}/(1 - \beta_2))$	$\checkmark$	$\checkmark$
$I_1(u - m_H^2, m_H^2 - u, -y_{2+}/\beta_2)$	$\times$	$\times$
$I_1(u - m_H^2, m_H^2 - u, -y_{2-}/\beta_2)$	$\checkmark$	$\times$

Table 1: Summary which term in  $D(p_1, p_2, p_3)$  leads to an imaginary part.  $\checkmark$  stands for a non-vanishing and  $\times$  for a vanishing imaginary part.

	(I)	(II)	(III)	(IV)
$I_2(m_q^2, m_H^2, y_{1+}/(1 - \beta_1))$	$\times$	$\checkmark$	$\times$	$\checkmark$
$I_2(m_q^2, m_H^2, y_{1-}/(1 - \beta_1))$	$\times$	$\checkmark$	$\times$	$\checkmark$
$I_2(m_q^2, u, -y_{1+}/\beta_1)$	$\times$	$\times$	$\times$	$\times$
$I_2(m_q^2, u, -y_{1-}/\beta_1)$	$\times$	$\times$	$\times$	$\times$
$I_2(m_q^2, s, \beta_2 + y_{2+})$	$\times$	$\checkmark$	$\times$	$\checkmark$
$I_2(m_q^2, s, \beta_2 + y_{2-})$	$\times$	$\checkmark$	$\times$	$\checkmark$
$I_2(m_q^2, m_H^2, y_{2+}/(1 - \beta_2))$	$\checkmark$	$\times$	$\checkmark$	$\times$
$I_2(m_q^2, m_H^2, y_{2-}/(1 - \beta_2))$	$\times$	$\checkmark$	$\times$	$\checkmark$
$I_2(m_q^2, m_H^2, -y_{2+}/\beta_2)$	$\checkmark$	$\times$	$\checkmark$	$\times$
$I_2(m_q^2, m_H^2, -y_{2-}/\beta_2)$	$\checkmark$	$\times$	$\checkmark$	$\times$

Table 2: Summary which term in  $D(p_1, p_2, p_3)$  leads to an imaginary part.  $\checkmark$  stands for a non-vanishing and  $\times$  for a vanishing imaginary part.

## References

- [1] A. Del Fabbro and D. Treleani. “Double parton scattering background to Higgs boson production at the CERN LHC”. In: *Phys. Rev. D* 61 (7 Mar. 2000), p. 077502. DOI: 10.1103/PhysRevD.61.077502. URL: <http://link.aps.org/doi/10.1103/PhysRevD.61.077502>.
- [2] A. Devoto and D.W. Duke. “Table of integrals and formulae for Feynman diagram calculations”. English. In: *La Rivista del Nuovo Cimento (1978-1999)* 7.6 (1984), pp. 1–39. DOI: 10.1007/BF02724330. URL: <http://dx.doi.org/10.1007/BF02724330>.
- [3] Markus Diehl, Daniel Ostermeier, and Andreas Schäfer. “Elements of a theory for multiparton interactions in QCD”. English. In: *Journal of High Energy Physics* 2012.3, 89 (2012). DOI: 10.1007/JHEP03(2012)089. URL: [http://dx.doi.org/10.1007/JHEP03\(2012\)089](http://dx.doi.org/10.1007/JHEP03(2012)089).
- [4] E.W.N. Glover and J.J. Van der Bij. “Z-boson pair production via gluon fusion”. In: *Nuclear Physics B* 321.3 (1989), pp. 561–590. ISSN: 0550-3213. DOI: [http://dx.doi.org/10.1016/0550-3213\(89\)90262-9](http://dx.doi.org/10.1016/0550-3213(89)90262-9). URL: <http://www.sciencedirect.com/science/article/pii/0550321389902629>.
- [5] E.W.N. Glover and J.J. van der Bij. “Higgs boson pair production via gluon fusion”. In: *Nuclear Physics B* 309.2 (1988), pp. 282–294. ISSN: 0550-3213. DOI: [http://dx.doi.org/10.1016/0550-3213\(88\)90083-1](http://dx.doi.org/10.1016/0550-3213(88)90083-1). URL: <http://www.sciencedirect.com/science/article/pii/0550321388900831>.